



Preparation and Characterization of Bulk and Alumina Supported Hausmannite Nanoparticles

N.M. DERAZ^{1*}, AHMED A. ABDELTAWAB^{2,3} and SALEM S. AL-DEYAB²

¹Physical Chemistry Department, Laboratory of Surface Chemistry and Catalysis, National Research Center, Dokki, Cairo, Egypt

²Chemistry Department, College of Science, King Saud University, Riyadh 11451, Saudi Arabia

³Chemical Engineering Department, Tabbin Institute for Metallurgical Studies, Cairo 11413, Egypt

*Corresponding author: E-mail: nmderaz@yahoo.com.

Received: 14 October 2013;

Accepted: 20 November 2013;

Published online: 22 March 2014;

AJC-14974

Bulk and alumina supported hausmannite Mn_3O_4 nano-particles were prepared by glycine assisted combustion method with different amounts of glycine. Scanning electron micrographs, energy dispersive X-ray and X-ray diffraction measurements display the structural and morphological properties of alumina and bulk and alumina supported hausmannite Mn_3O_4 nano-particles. The as prepared systems are spongy, homogeneous and fragile. XRD results showed alumina in all samples is amorphous phase. However, the produced manganese oxide is hausmannite Mn_3O_4 with spinel structure. The change in the amount of glycine and using of alumina carrier led to a significant change in the crystallite size, lattice constant and unit cell volume of Mn_3O_4 phase.

Keywords: XRD, SEM, EDX, Hausmannite Mn_3O_4 nano-particles.

INTRODUCTION

Tetragonal manganese oxide, (hausmannite Mn_3O_4) can be crystallized in the normal spinel structure with a tetragonal distortion elongated along the c-axis. The cation distribution of Mn ions in the spinel structure showed that divalent manganese ions are located in the tetrahedral A-sites and trivalent manganese ions are located in octahedral B-sites¹. Mn_3O_4 is one of the most stable oxides of manganese due to its wide range of technological applications such as high-density magnetic storage media, catalysts, ion exchange, molecular adsorption, electrochemical materials, corrosion-inhibiting pigment, batteries, varistors, solar energy transformation, electronics and information technology²⁻⁴.

Indeed, Mn_3O_4 is active catalyst for various catalytic reactions such as the decomposition of NO_x released from internal engines and the oxidation of both C_6H_6 and CO_2 ^{5,6}. Mn-Fe oxides composite is suitable catalyst for drinking water treatment process depending upon remarkable phosphorus removal efficiency⁷. Mn_3O_4 can be used as an anode for lithium-ion batteries because it is inexpensive and environmentally benign. However, this oxide has a high theoretical specific capacity and lower electrical conductivity compared with other oxides^{8,9}. Mn_3O_4 is one of the most promising electrode materials for commercial super-capacitors due to unique properties. These properties are good efficiency, better stability, high abundance and relatively broad work potential window in aqueous solution¹⁰⁻¹².

Mn_3O_4 has large surface area and different morphology. In other words, Mn_3O_4 has various forms and shapes such as nano-rods, nano-wires, tetragonal, polyhedral nano-crystals, sphere-like nano-crystals and nano-particles¹³⁻¹⁸. The performance of Mn_3O_4 in the previous application depends on the structural and morphological properties. The preparation method of Mn_3O_4 is the important factor to control in the previous properties. The traditional method to prepare of Mn_3O_4 was ceramic method *via* heating of manganese oxides or manganese hydroxides, oxyhydroxide, nitrate, sulfate and carbonate at about 1000 °C in air¹⁹⁻²¹. However, various methods were used to prepare Mn_3O_4 such as solvothermal/hydrothermal, vapor phase growth, vacuum calcinating precursors, thermal decomposition, ultrasonic, γ - and microwave irradiation and chemical liquid homogeneous precipitation²²⁻²⁹.

This study is focused on the effect of glycine as fuel on the formation of bulk and alumina supported hausmannite manganese nano-particles. However, the structural and morphological properties of the as prepared system have been determined. Different techniques were used for characterization of the as synthesized systems.

EXPERIMENTAL

Preparation of the as prepared systems: One sample of Mn oxide was prepared by mixing calculated amount of glycine and manganese nitrate. The mixed precursors were concentrated in a porcelain crucible on a hot plate at 400 °C

for 15 min. The crystalline water was gradually vaporized during heating and when a crucible temperature was reached, a great deal of foams produced and spark appeared at one corner which spread through the mass, yielding a voluminous and fluffy product in the container. In this research, the ratio of glycine: manganese nitrate was 4:1 for S1 sample. In addition, two samples of alumina supported manganese were prepared by the same method with ratio of (4 and 8) glycine: (1) manganese: (2) aluminum nitrate for S2 and S3 samples, respectively. The chemicals employed in the present work were of analytical grade supplied by Prolabo Company. A general flowchart of the synthesis process is shown in Fig. 1.

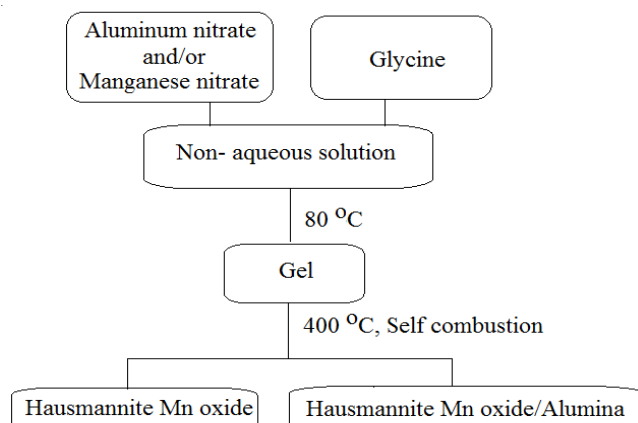


Fig. 1. Process flowchart for fabricating the as prepared samples

Characterization: An X-ray measurement of various mixed solids was carried out using a BRUKER D8 advance diffractometer (Germany). The patterns were run with $\text{CuK}\alpha$ radiation at 40 kV and 40 mA with scanning speed in 2θ of 2°min^{-1} . The crystallite size of CuMn_2O_4 present in the investigated solids was based on X-ray diffraction line broadening and calculated by using Scherrer equation³⁰.

$$d = \frac{B\lambda}{\beta \cos\theta} \quad (1)$$

where d is the average crystallite size of the phase under investigation, B is the Scherrer constant (0.89), λ is the wave length of X-ray beam used, β is the full-width half maximum (FWHM) of diffraction and θ is the Bragg's angle.

Scanning electron micrographs (SEM) was recorded on JEOL JAX-840A electron micro-analyzer. The sample was dispersed in ethanol and then treated ultrasonically in order to disperse individual particles over gold grids.

Energy dispersive X-ray analysis (EDX) was carried out on Hitachi S-800 electron microscope with an attached keveX Delta system. The parameters were as follows: accelerating voltage 15 kV, accumulation time 100s, window width 8 μm . The surface molar composition was determined by the Asa method, Zaf-correction, Gaussian approximation.

RESULTS AND DISCUSSION

X-ray diffraction: On the basis of the preliminary experiments and on earlier studies, the thermal treatment of manganese nitrate on hotplate at 400 °C for 15 min. resulted in formation of a mixture of MnO_2 (pyrolusite and/or γ -phase

as a major phase) and Mn_2O_3 (bixbyite as a minor phase). However, the relative abundance of MnO_2 was more pronounced compared to that of Mn_2O_3 ³¹. X-Ray diffractograms for the as prepared samples are given in Fig. 2.

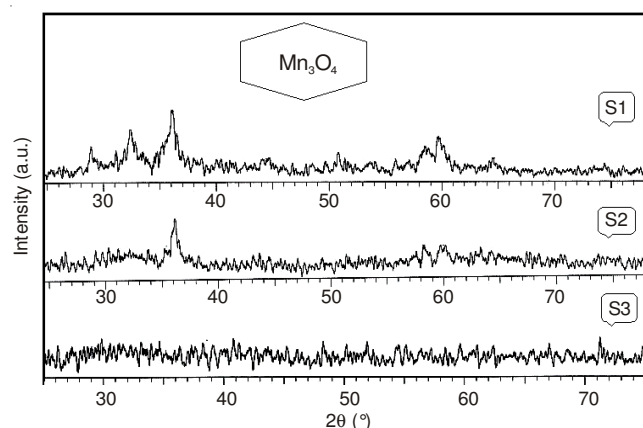


Fig. 2. XRD pattern for the S1, S2 and S3 samples

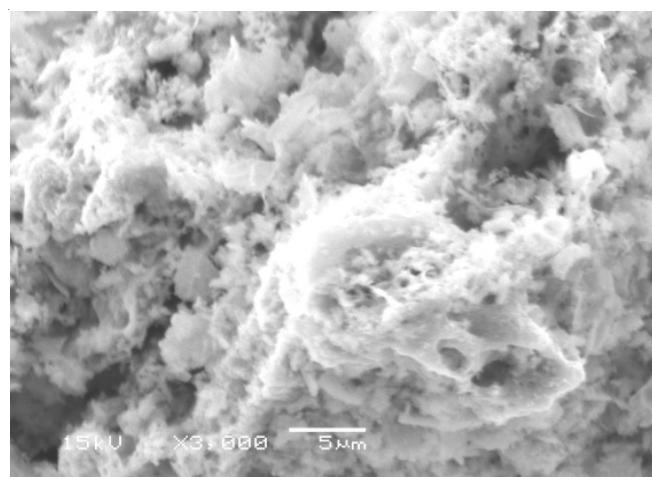
Examination of Fig. 2 resulted in some observations are summarized as following: (i) The pattern of S1 sample contains all diffraction line relative to Mn_3O_4 phase (hausmannite, space group I41amd(141), JCPDS No.80-0382). This phase is observed as a single phase with low crystallinity. In fact, Mn_3O_4 phase has tetragonal spinel structure with different planes (1 1 2), (2 0 0), (1 0 3), (2 1 1), (0 0 4), (2 2 0), (1 0 5), (3 1 2), (3 0 3), (3 2 1), (2 2 4) and (3 1 4). (ii) Although the S1 sample contains a mixture of Mn and Al oxides, it was found that the XRD pattern of this sample displays final product containing a moderate crystalline Mn_3O_4 phase as a single phase. In other words, coexistent of Mn and Al oxides resulted in a decrease in the crystallinity of Mn_3O_4 phase as shown in the S₂ sample. Increasing the amount of glycine brought about a significant decrease in the crystallinity of Mn oxide as shown in the S₃ sample. Indeed, the S₃ sample consisted of amorphous oxides indicating the effect of amount of glycine content in the preparation process. The calculated values of the crystallite size (d), lattice constant (a), unit cell volume (V) and X-ray density (D_x) of Mn_3O_4 phase, depending upon the data of X-ray, are given in Table-1.

TABLE-1
CRYSTALLITE SIZE AND LATTICE
PARAMETERS OF Mn_3O_4 PHASE

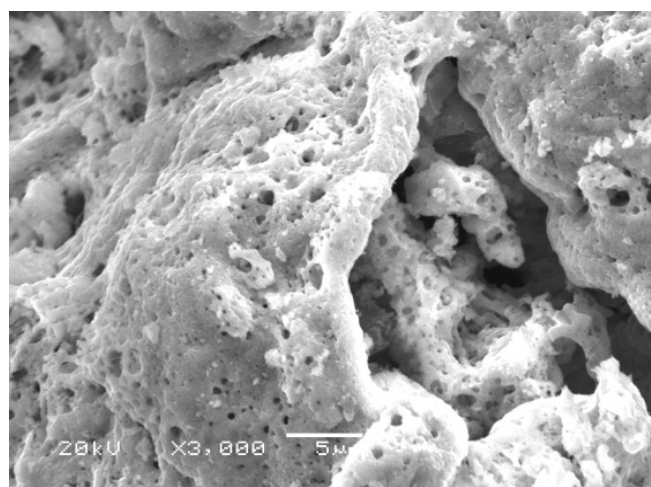
Samples	Mn_3O_4				
	d (nm)	a (nm)	b (nm)	c (nm)	V (nm^3)
S2	37	0.5767	0.5767	0.9452	3.1458
S3	26	0.5752	0.5752	0.9421	3.1434

SEM study: Scanning electron micrographs (SEM) can be used for study the morphology of the S1, S2 and S3 samples as shown in Fig. 3 A-C. Investigation of this figure found that the as synthesized solids are spongy, homogeneous and fragile material. However, liberation of large amount of gases during combustion process resulted in appearance of voids and pores in the solids studied.

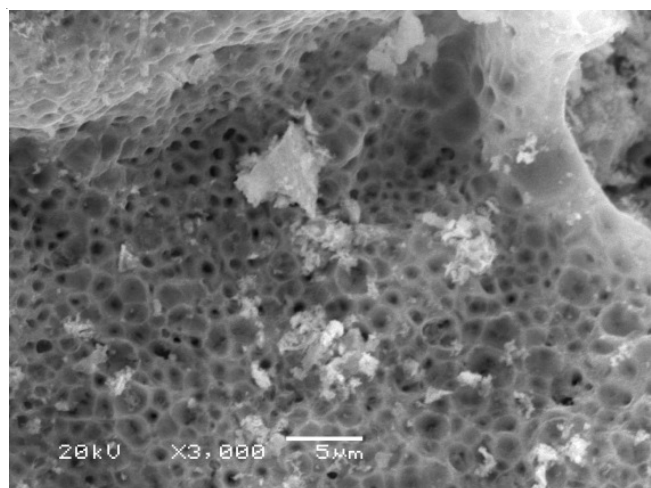
EDX measurements: Fig. 4 showed EDX measurements of the as prepared systems at 20 keV. These measurements



(A)



(B)



(C)

Fig. 3. SEM images for the as prepared samples; (A) S1, (B) S2 and (C) S3

showed the effective atomic concentrations of different constituents involved in the S1, S2 and S3 samples studied.

Homogeneity of elements: EDX technique enables us to study the homogeneity of elements in the as prepared samples. Table-2 displays that the concentrations of different

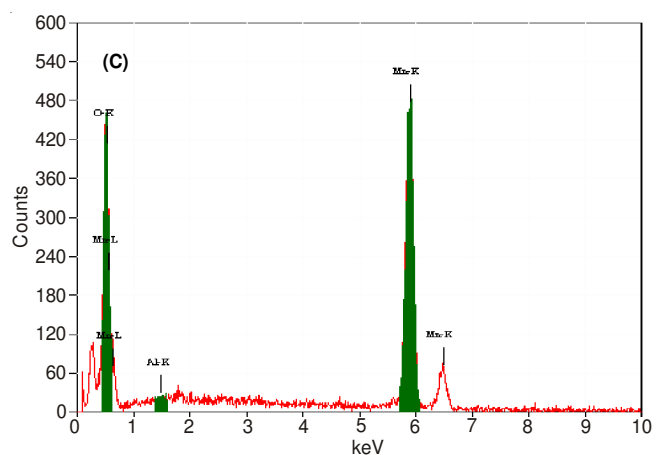
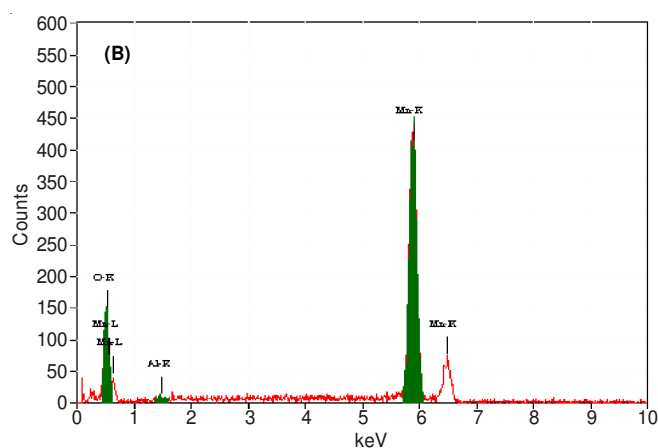
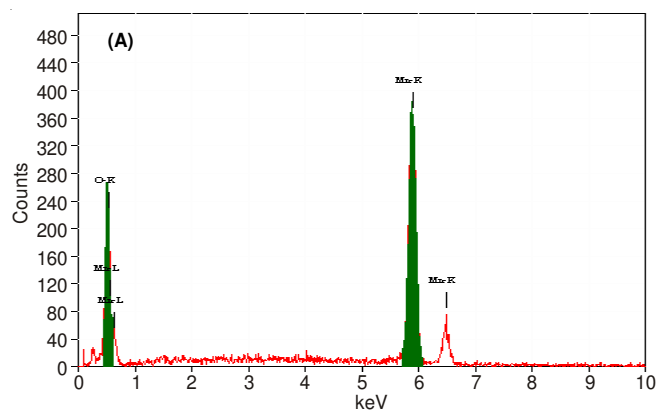


Fig. 4. EDX spectrum for the as prepared samples; (A) S1, (B) S2 and (C) S3

constituents at different points over every solid are very close to each other indicating the homogeneity of the as prepared systems.

Element gradient: In addition, determination of the concentrations of O, Mn and Al species from the uppermost surface to the bulk layers of the S1, S2 and S3 can be calculated using EDX technique at 15 and 20 keV. The obtained results showed that the surface concentrations of Mn and oxygen species for the as prepared samples have the same values at different applied voltages. This observation suggests a good distribution for the elements with formation of Mn-Al-O solid solution.

Glycine- assisted combustion route is a simple one-step and "green" strategy for the synthesis of Mn_3O_4 , alumina and Mn_3O_4 - alumina composite. This route features environmental

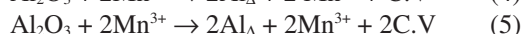
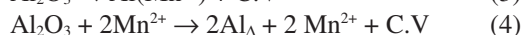
TABLE-2
ATOMIC ABUNDANCE OF ELEMENTS MEASURED AT 20 keV
AND DIFFERENT AREAS OVER THE S1, S2 AND S3 SAMPLES

Samples	Elements	Point 1	Point 2	Point 3
S1	O	22.55	22.55	22.25
	Mn	77.45	77.45	77.45
S2	O	22.55	22.58	22.67
	Mn	77.45	77.37	77.07
	Al	0	0.05	0.25
S3	O	22.67	22.62	22.56
	Mn	77.08	77.24	77.73
	Al	0.25	0.14	0.22

benignity, high yield, inexpensive and high safety. Indeed, the traditional method for preparation of Mn_3O_4 (hausmannite) phase is the ceramic method *via* thermal treatment of Mn_2O_3 phase at elevated temperatures³². However, Mn_2O_3 phase can be prepared from the thermal treatment of MnO_2 at temperature starting from 600 °C³². In fact, the preliminary experiments showed that a mixture of Mn_2O_3 and MnO_2 can be formed by heating of Mn nitrate on hotplate at 400 °C. In this study, the heat treatment of a mixture of calculated amounts of both manganese nitrate and glycine (as a fuel) at 400 °C on hotplate resulted in formation of moderate crystalline Mn_3O_4 (hausmannite) as a single phase without any indication for other crystalline byproducts such as MnO or Mn_2O_3 .

The co-existence of Mn and Al oxides brought about a decrease in the crystallite size and lattice parameter of Mn_3O_4 phase. This decrease depends on the glycine content. In other words, the presence of 4 mole of glycine led to a decrease of crystallite size of Mn_3O_4 from 37 nm to 26 nm. However, using of 8 mole glycine resulted in amorphous Mn_3O_4 crystallites indicating a drastic decrease in the crystallite size of this phase. This indicates the important role of alumina in increasing of the dispersion of manganese species on its surface. The decrease in the crystallite size and/or the lattice parameter could be attributed to the difference in the ionic radii of Mn and Al species. In fact, the ionic radius of Al^{3+} ions (0.050 nm) is smaller than that of Mn ions ($Mn^{2+} = 0.076$ nm and $Mn^{3+} = 0.063$ nm)³². Consequently, some Al species can be incorporated in the Mn oxide lattices yielding contraction in these lattices.

The dissolution of Al^{3+} ions in the lattices of Mn_2O_3 and/or Mn_3O_4 can be proceed *via* substitution of some host Mn^{2+} and Mn^{3+} ions and/or also by their location in interstitial positions forming solid solution. The dissolution process can be simplified by the use of Kröger's notations³³ in the following manner:



$Al(Mn^{2+})$ and $Al(Mn^{3+})$ are the trivalent aluminium ions located in the positions of host manganese oxides in Mn_2O_3 and/or Mn_3O_4 ; Al_{Δ} is aluminium ions located in the interstitial positions of manganese oxide lattices; C.V. created cationic vacancies. The dissolution of some Al ions in the lattices of manganese oxides according to the previous reactions (2, 3, 4 and 5) which led to creation of cationic vacancies might increase the mobility of cations of reacting oxides (Mn^{2+} and Mn^{3+})

with subsequent an increase in the dispersion of Mn species on the alumina surface.

SEM and EDX measurements showed that glycine-assisted combustion route is simple method for preparation of bulk and supported manganese spinel solids. These solids are fragile, spongy and homogeneous. However, the results of EDX confirm formation of Al_2O_3 , Mn_3O_4 and Mn_3O_4/Al_2O_3 solids with low crystallite size. These observations are consistent with the results of XRD.

Conclusions

Mn_3O_4 and Mn_3O_4/Al_2O_3 systems can be prepared by glycine-assisted combustion method. This method resulted in high yield for the final products. However, these materials are spongy, homogenous and fragile. The crystallite size, lattice constant and unit cell volume and nano-crystalline particles were calculated depending upon the X-ray data. Nano-crystalline phase in all system is hausmannite Mn_3O_4 . It was found that the increase in amount of glycine led to a decrease in the crystallite size and lattice parameters of Mn_3O_4 phase. In other words, the incorporation of some Al species in Mn lattices led to formation of point defects in hausmannite structure with subsequent changes in the lattice parameter.

ACKNOWLEDGEMENTS

This project was supported by King Saud University, Deanship of Scientific Research, College of Science Research Centre.

REFERENCES

1. E. Karaoglu, H. Deligoz, H. Sozeri, A. Baykal and M.S. Toprak, *Nano-Micro Lett.*, **3**, 25 (2011).
2. Y. Yamashita, K. Mukai, J. Yoshinobu, M. Lippmaa, T. Kinoshita and M. Kawasaki, *Surf. Sci.*, **514**, 54 (2002).
3. A.H. de Vries, L. Hozoi, R. Broer and P. Bagus, *Phys. Rev. B*, **66**, 035108 (2002).
4. A.H. de Vries, L. Hozoi, R. Broer and P. Bagus, *Phys. Rev. B*, **66**, 035108 (2002).
5. H. Einaga and S. Futamura, *J. Catal.*, **227**, 304 (2004).
6. P. Lidström, J. Tierney, B. Wathey and J. Westman, *Tetrahedron*, **57**, 9225 (2001).
7. Y.L. Yang, X. Li, C.X. Guo, F.W. Zhao and F. Jia, *Chem. Res. Chin. Univ.*, **25**, 224 (2009).
8. X. Fang, X. Lu, X. Guo, Y. Mao, Y.-S. Hu, J. Wang, Z. Wang, F. Wu, H. Liu and L. Chen, *Electrochem. Commun.*, **12**, 1520 (2010).
9. Y. Li, H. Tan, X.-Y. Yang, B. Goris, J. Verbeeck, S. Bals, P. Colson, R. Cloots, G. Van Tendeloo and B.-L. Su, *Small*, **7**, 475 (2011).
10. B.Q. Jiang, Y. Liu and Z.B. Wu, *J. Hazard. Mater.*, **162**, 1249 (2009).
11. S.-B. Ma, K.-W. Nam, W.-S. Yoon, S.-M. Bak, X.-Q. Yang, B.-W. Cho and K.-B. Kim, *Electrochem. Commun.*, **11**, 1575 (2009).

12. X.Q. Yu, Y. He, J.P. Sun, K. Tang, H. Li, L.Q. Chen and X.J. Huang, *Electrochem. Commun.*, **11**, 791 (2009).
13. Z.H. Wang, D.Y. Geng, Y.J. Zhang and Z.D. Zhang, *J. Cryst. Growth*, **310**, 4148 (2008).
14. Y.C. Zhang, T. Qiao and X. Ya Hu, *J. Solid State Chem.*, **177**, 4093 (2004).
15. M. Anilkumar and V. Ravi, *Mater. Res. Bull.*, **40**, 605 (2005).
16. L.X. Yang, Y.J. Zhu, H. Tong, W.W. Wang and G.F. Cheng, *J. Solid State Chem.*, **179**, 1225 (2006).
17. K.A.M. Ahmed, Q. Zeng, K. Wu and K. Huang, *J. Solid State Chem.*, **183**, 744 (2010).
18. Y.Q. Chang, X.Y. Xu, X.H. Luo, C.P. Chen and D.P. Yu, *J. Cryst. Growth*, **264**, 232 (2004).
19. J. Zhang, J. Du, H. Wang, J. Wang, Z. Qu and L. Jia, *Mater. Lett.*, **65**, 2565 (2011).
20. F. Giovannelli, C. Autret-Lambert, C. Mathieu, T. Chartier, F. Delorme, A. Seron, *J. Solid State Chem.*, **192**, 109 (2012).
21. C. Chen, G.J. Ding, D. Zhang, Z. Jiao, M.H. Wu, C.H. Shek, C.M.L. Wu, J.K.L. Lai and Z. Chen, *Nanoscale*, **4**, 2590 (2012).
22. Y.C. Zhang, T. Qiao and X. Ya Hu, *J. Solid State Chem.*, **177**, 4093 (2004).
23. Y.Q. Chang, D.P. Yu, Y. Long, J. Xu, X.H. Luo and R.C. Ye, *J. Cryst. Growth*, **279**, 88 (2005).
24. J. Du, Y. Gao, L. Chai, G. Zou, Y. Li and Y. Qian, *Nanotechnology*, **17**, 4923 (2006).
25. M. Salavati-Niasari, F. Davar and M. Mazaheri, *Polyhedron*, **27**, 3467 (2008).
26. I.K. Gopalakrishnan, N. Bagkar, R. Ganguly and S.K. Kulshreshtha, *J. Cryst. Growth*, **280**, 436 (2005).
27. Y. Hu, J. Chen, X. Xue and T. Li, *Mater. Lett.*, **60**, 383 (2006).
28. S.K. Apte, S.D. Naik, R.S. Sonawane, B.B. Kale, N. Pavaskar, A.B. Mandale and B.K. Das, *Mater. Res. Bull.*, **41**, 647 (2006).
29. Z.W. Chen, J.K.L. Lai and C.H. Shek, *Appl. Phys. Lett.*, **86**, 181911 (2005).
30. B.D. Cullity, *Elements of X-ray Diffraction*, Addison-Wesley Publishing Co. Inc., Ch. 14 (1976).
31. R. Craciun, *Catal. Lett.*, **55**, 25 (1998).
32. N.-A.M. Deraz, M.A. El-Sayed and A.A. El-Aal, *Adsorp. Sci. Technol.*, **19**, 541 (2001).
33. F.A. Kroger, *Chemistry of Imperfect Crystals*, North-Holland, Amsterdam (1964).